

Purification of an Industrial Aluminum Alloy by Melt Stirring During Ohno Continuous Casting Process

Simbarashe FASHU*, Li JIANGUO and Hu Qiao DAN

*School of Material Science and Engineering,
Shanghai Jiao Tong University, Shanghai, 200240, China*

Abstract

With the purpose of upgrading the purity of a dilute industrial aluminum alloy during Ohno Continuous Casting (OCC) process through the use of forced melt stirring; the critical stirring intensity required under a casting speed of 2 mm/min was numerically determined. The determined critical stirring intensity induces convective velocity magnitudes into the melt which are effective in transporting solutes from the solute boundary layer into the bulk melt. It was found that, with adequate melt stirring, production of substantially long and high purity ingots during OCC is possible before their purity diminishes to lower than the initial alloy purity.

Key words: Segregation, Impurities, Computer Simulation, Purification, Stirring

Introduction

The mode of redistribution of excess solutes accumulating at the solid-liquid interface during Ohno Continuous Casting (OCC) is a key factor determining the final purity of the produced ingots⁽¹⁾. In absence of adequate melt convection, the rejected solutes forms a thick enriched solute boundary layer at the solid-liquid interface upon which solute transport is solely through diffusion⁽²⁾. Thus, purification of the ingot occurs only during the transient stage before the accretion of the solute boundary layer at the stationary solid-liquid interface and after that the solid will maintain the initial composition of the alloy due to a high solute concentration in the liquid at the interface⁽³⁾. In order to obtain high purity ingots during OCC process, a sufficiently strong convection towards the solidification front reduces the thickness of the boundary layer⁽⁴⁾, thus lowering solute concentration in the solid. Purification of metals during solidification by taking advantage of segregation and melt convection is now an established process and is more effective if the partition coefficients of solutes are much less than unity. Mullin and Hulme⁽⁵⁾ in 1958 equipped the zone refining process with an alternating magnetic field and obtained an enhanced purification rate in zone refining of semiconductors due to forced melt mixing. The emphasis of this article is placed upon using computer simulation to determine the adequate mechanical critical melt stirring intensity required under a casting speed of 2 mm/min during

OCC of aluminum rods to produce ingots of high purity. The lower casting speed (solidification rate) is used to increase the size of the mushy zone and the time for the solute rich liquid in the mushy zone to flow.

Brief Introduction of OCC Process

Ohno Continuous Casting (OCC) process is a recently developed heated mold unidirectional continuous casting process used for producing superior, unidirectional rods and wires of substantial length^(6,7). High quality wires are formed by maintaining the solid-liquid interface outside the heated mold and an axial temperature gradient between the cooling region and heated mold, thus avoiding solidification in the mold⁽⁸⁾. The process is reliable in producing high purity wires and rods required mostly for the telecommunications industry and modern science technology e.g. video and audio cables⁽⁶⁾. As shown schematically in Figure 1, the OCC process involves the continuous introduction of molten metal into an externally heated mould which is held slightly above the melting point of the metal being cast; heat is extracted from the cast product by means of a cooling device located some distance from the mould exit. The solidified ingot is pulled with the pinch rollers placed some distance from the water cooling region.

*Corresponding author E-mail: sfashu04@gmail.com

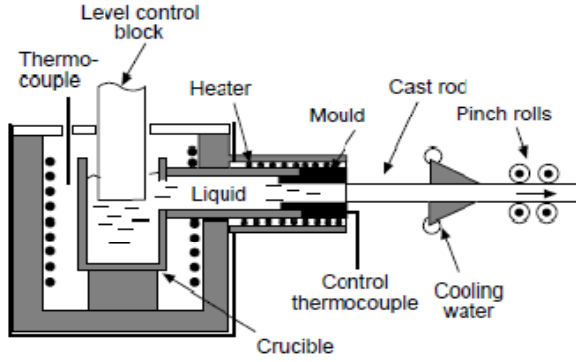


Figure 1. Schematic diagram of the horizontal OCC process.

Mathematical Model

Mechanical Stirring OCC Configuration

The OCC domain considered in our simulation is shown in Figure 2 and the regions of interest are the liquid in the heated mold and solid ingot, surrounding the solid-liquid interface where solidification and mass transfer occur.

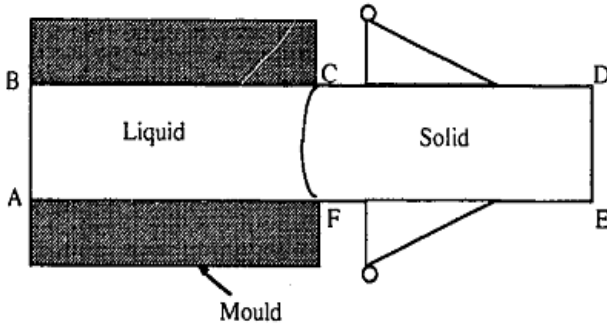


Figure 2. OCC domain considered in simulation.

Melt stirring was induced into the melt through mechanical rotation of a stirrer positioned at 30 mm from the mold exit as shown in Figure 3 to produce an effective axial flow field required for solute transport.

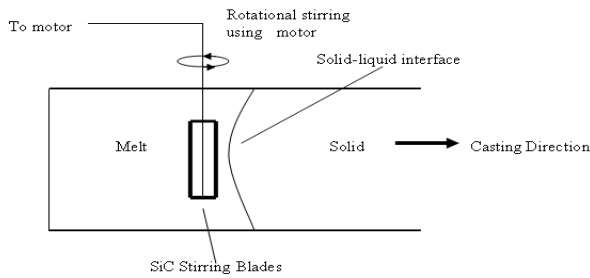


Figure 3. Positioning of a stirring blade in the melt near the interface for stirring.

Governing Equations

A macro-transfer model, based on the continuum model of Benon and Incropera⁽⁹⁾ and reassessed by Prescott et al.⁽¹⁰⁾ was used for predicting the solute distribution during OCC of a multicomponent alloy.

Assumptions:

1. All of the properties of the mixture can be obtained from the properties of its components in each phase.
2. All transport properties of each phase, such as thermal and electrical conductivity or viscosity, are constants.
3. The density is constant in each phase and the densities of the two phases are similar.
4. The mushy region is modeled by means of using the mixture viscosity.
5. Local equilibrium is assumed to exist at the solid-liquid interface i.e. the phase diagram is applied i.e. $C_{i,sol} = K_i C_{i,liq}$.
6. The flow of the liquid phase is assumed to be incompressible, laminar and Newtonian.
7. Solutes diffusion coefficients are anisotropic and constant in each phase.

Based on the assumptions made above, the set of governing equations of heat, momentum and solute transport are:

Mass Conservation Equation:

$$\frac{\partial \rho}{\partial t} + \nabla \cdot (\rho \vec{u}) = 0 \quad (1)$$

Where t is the time, ρ is the density, \vec{u} is the average velocity of the mixture, which can be defined as $\vec{u} = f_s \vec{u}_s + f_l \vec{u}_l$ where f_s and f_l are solid and liquid fractions, respectively.

Momentum Conservation Equation:

$$\frac{\partial (\rho \vec{u})}{\partial t} + \nabla \cdot (\rho \vec{u} \vec{u}) = -\nabla p + \nabla \cdot (\mu_l \nabla \vec{u}) - \frac{(1-f_l)^2}{(f_l + \epsilon)^3} (\vec{u} - \vec{u}_s) A_{mush} + S_m \quad (2)$$

where p is the pressure, μ_l is the dynamic viscosity of the melt, K is the permeability constant of the mushy zone, ϵ is a small number (0.001) to prevent division by zero, u_s is the solid velocity due to ingot pulling, S_m is the momentum source which is only due to mechanical stirring in this case. The enthalpy-porosity technique was used to treat the

*Purification of an Industrial Aluminum Alloy by Melt Stirring During
Ohno Continuous Casting Process*

mushy zone as a pseudo porous medium, with the porosity of each cell being set to its liquid fraction. The variation of permeability is approximated as function of liquid mass fraction f_l using the Carman-Kozeny relation:

$$K = K_0 \frac{f_l^3}{(1-f_l)^2} \quad (3)$$

Where K_0 is a permeability constant depending on the morphology of the two-phase mushy region.

$A_{mush} = \frac{\mu_l}{K_0}$ is the mushy zone constant and depends on the material. The value of K_0 is usually approximated as $K_0 = \frac{d^2}{180}$, where d denotes the dendrite arm spacing.

Energy Conservation Equation:

$$\frac{\partial(\rho H)}{\partial t} + \nabla \cdot (\rho H \vec{u}) = \nabla \cdot (k \nabla T) + S_h \quad (4)$$

Where H is enthalpy, k is thermal conductivity; T is temperature and the source term, S_h can be written as:

$$S_h = -\nabla \cdot [\rho(H_l - H)(\vec{u} - \vec{u}_s)]$$

The first term on the right hand side of Eq(4) represent the net Fourier diffusion flux. The enthalpy was computed as the sum of the sensible enthalpy, h , and the latent heat, ΔH :

$$H = h + \Delta H \quad (5)$$

Where

$$h = h_{ref} + \int_{T_{ref}}^T C_p dT \quad (6)$$

Where h_{ref} =reference enthalpy, T_{ref} =reference temperature, C_p =specific heat at constant pressure. The latent heat content written in terms of the latent heat of the material, L is:

$$\Delta H = f_l L \quad (7)$$

The latent heat content can vary between zero (for a solid) and L (for a liquid) and f_l is obtained from equation 8.

The liquid fraction is assumed to be linearly (Lever rule) proportional to temperature as:

$$f_i = \begin{cases} 1 & \text{when } T \geq T_l \\ \frac{T - T_s}{T_l - T_s} & \text{when } T_l \geq T \geq T_s \\ 0 & \text{when } T \leq T_s \end{cases} \quad (8)$$

Assuming that the solidus and liquidus lines are straight lines, the solidus and liquidus temperatures of a species mixture can be expressed as:

$$T_{liq} = T_{melt} + \sum_{i=1}^n m_i C_i \quad (9)$$

$$T_{sol} = T_{melt} + \sum_{i=1}^n \frac{m_i C_i}{k_i} \quad (10)$$

Where T_m is the fusion temperature, m_i is the slope of the liquidus surface with respect to solute i and aluminum and k_i is the partition coefficient of solute i . The solution for temperature is essentially an iteration between the energy Eq(4) and the liquid fraction Eq(7) using the method suggested by Voller and Swaminathan⁽¹¹⁾ to update the liquid fraction.

Solute Conservation Equation:

$$\frac{\partial(\rho C_i)}{\partial t} + \nabla \cdot (\rho [f_l u_l C_{i,l} + (1-f_l) u_c C_{i,s}]) = \nabla \cdot [f_l D_{i,m,l} \nabla C_{i,l} + (1-f_l) \rho D_{i,m,s} \nabla C_{i,s}] + S_c \quad (11)$$

Where, C_i is the total mass fraction of species i , $C_i = f_s C_s^i + f_l C_l^i$, D is the diffusion coefficient, $S_c = -\nabla \cdot [\rho(C_l^i - C_i)(\vec{u} - \vec{u}_s)]$ is the advection source term in the mushy zone due to the relative phase motion. The subscripts i, l, c, m and s represents the species number, liquid, casting, mixture and solid respectively. u_l is the velocity of the liquid and u_c is the casting velocity imparted on the ingot by the pinch rollers. The term on the right hand side of Eq(11) represents the net Fickian diffusion flux of solutes associated with the solid and liquid phases. The liquid velocity, u_l is found from the average velocity as follows:

$$\vec{u}_l = \frac{(\vec{v} - \vec{v}_s f_s)}{f_l} \quad (12)$$

The mixture quantities are defined in the following manner:

$$f_l + f_s = 1, \quad H = H_l f_l + H_s f_s, \quad D = D_l f_l + D_s f_s, \quad k = k_l f_l + k_s f_s$$

With the microscopic consideration of local equilibrium in the mushy zone, the energy and species conservation equations are closed using the equilibrium phase diagram and the liquid fraction in the whole domain, f_l is defined by the Lever rule as shown in Eq(7). The assumption of local equilibrium at the interface does not preclude the existence of non-equilibrium conditions on a macroscopic scale, which are catered for in the macroscopic Eq(9).

Numerical Solution

The generalized format of the governing equations contains the transient terms, convective terms, diffusion terms and source terms, hence the numerical procedure of solving them only requires slight modifications for the format of source terms as suggested by Patankar⁽¹²⁾. The solidification model was introduced and solved iteratively in CFD Fluent 6.3.26 software through the aid of User Defined Subroutines and convenient source terms of governing equations were introduced through User Defined Functions (UDFs). A fully implicit control volume based formulation was used for the time dependent terms, and the combined convection/diffusion coefficients were discretized using an upwind scheme. In order to resolve the pressure-velocity coupling in the momentum equations the SIMPLE algorithm was used and pressure was

discretized by the PRESTO! method. A momentum source term due to mechanical stirring was introduced into the melt through Multiple Reference Frame (MRF) model. A full two dimensional single domain, fixed uniform grid of Figure 2 was used for the numerical calculation. Because of the high nonlinearity and full coupled nature of the governing equations, under-relaxation factors were reduced accordingly to obtain converged solutions. Double-diffusive convection in the melt was intentionally neglected in order to test theoretical models for diffusive regime and compare them with simulation results of solute redistribution in absence of melt convection. Furthermore, the alloy is dilute such that solutal diffusion is negligible, and the use of a heated mold in horizontal OCC with gravity vector being perpendicular to thermal gradient makes thermal convection effects to be insignificant⁽¹³⁾.

The industrial aluminum alloy used is composed of copper and silicon as major impurities. Thermo-physical properties of the industrial dilute aluminum alloy and the initial and boundary conditions used in this simulation are shown in Table 1 and Table 2 respectively. The solid-liquid interface position was controlled to be just near the stirring blades through adjustment of cooling in the water spray region.

Table 1. Thermo physical properties of Al 0.12wt%Cu 0.11wt%Si alloy.

Property	Units	Symbol	Values
Density of liquid	kg/m^3	ρ	2400 ⁺
Density of solid	kg/m^3	ρ	2660 ⁺
Specific heat	J/kgK	C_p	1080 ⁺
Thermal conductivity of liquid	w/mK	K_s	90 ⁺
Thermal conductivity of solid	w/mK	K	180 ⁺
Diffusion coefficient of Cu in liquid	m^2/s	$D_{L,Cu}$	6e-9 ⁺
Diffusion coefficient of Si in liquid	m^2/s	$D_{L,Si}$	4e-9 ⁺
Diffusion coefficient of Cu in solid	m^2/s	$D_{s,Cu}$	5e-13 ⁺
Diffusion coefficient of Si in solid	m^2/s	$D_{s,Si}$	3e-13 ⁺
Partition coefficient of Cu in Al	-	k	0.14 ⁺
Partition coefficient of Si in Al	-	k	0.13 ⁺
Melting temperature of Al	K	T	933 ⁺
Slope of liquidus line Al-Cu	-	m	-3.43 ⁺
Slope of liquidus line Al-Si	-	m	-6 ⁺
Viscosity of melt	Pas	μ	0.0013 ⁺
Melting heat	kJ	L	390 ⁺

*Purification of an Industrial Aluminum Alloy by Melt Stirring During
Ohno Continuous Casting Process*

Table 2. Initial and boundary conditions.

Property	Unit	Value
Melt Inlet temperature	K	938
Melt inlet velocity	mm/min	2
Ingot pulling speed	mm/min	2
Heat transfer coefficient of Al in air	w/m^2k	414
Heat transfer coefficient of Al in water spray	w/m^2k	10000-50000
Temperature of heated mold	K	938

Simulation Results and Discussion

Validation of Solidification Results with Published Literature

In order to validate the solidification model which was used in our computations, the model was compared against theory and experimental results from literature. Lee et al.⁽¹⁴⁾ used Bridgman growth to grow ingots of 0.4 mm and 5.5 mm diameter in absence of external melt convection using Al4wt%Cu at a casting speed of 0.4 μ m/s and produced 40 mm ingots during transient state before the solute boundary layer had sufficient time to build. The Electron Microprobe Analysis (EMPA) composition profile of short solid samples and liquid was done as shown in Figure 4.

Simulation to show the capability of the solidification model was done using the same conditions as those used by Lee et al.⁽¹⁴⁾. Figure 4 shows the simulated copper solute redistribution after OCC of 5.5 mm ingots during the transient state. This result is in good agreement with experimental results obtained by Lee et al.⁽¹⁴⁾ as shown in Figure 4 showing that the model is capable of computing solute redistribution at the casting speeds considered. The solid solute composition obtained in simulation (Figure 5) is almost the same as that obtained in experimental results (Figure 4) showing the capability of the model to predict the solute redistribution.

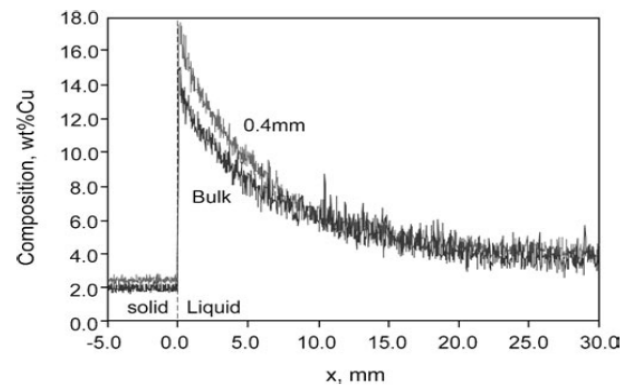


Figure 4. Line scan EPMA result of the composition profiles in 0.4 mm and 5.5 mm (bulk) diameter and 40 mm long ingots of Al-4wt% Cu alloy unidirectionally solidified with bridgman furnace at 0.4 μ m/s⁽¹⁴⁾.

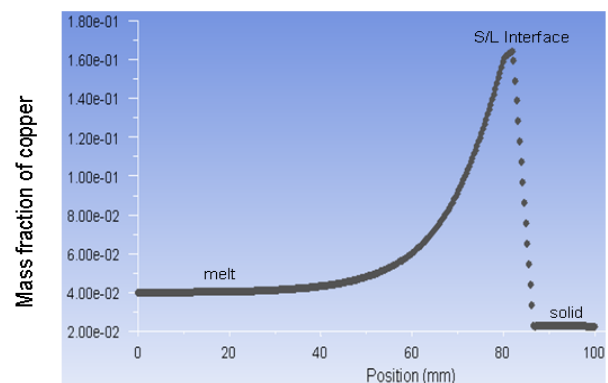


Figure 5. Solute redistribution obtained by simulation using experimental conditions from Lee et al.⁽¹⁴⁾.

Solidification and Mechanical Stirring Results

Figure 6 shows the temperature distribution profile of the solidification during the OCC process. The solidus and liquidus fronts are almost stationary and solidification starts at the centre of the ingot.

Figure 7 shows the aluminum redistribution after the OCC process has reached steady state in composition when there is no fluid flow and the solute distribution is caused only by the diffusion mechanism. This is in agreement with the theory from Tiller⁽³⁾, which states that the solute redistribution is constant once steady state condition is attained.

Figure 8 shows the corresponding axial aluminum redistribution near the center of the ingot. Purification of the ingot occurs during the transient process before the solute boundary layer is established. Using unsteady state simulation, it was found that about 500 mm ingots were cast to reach that state in composition. After attaining steady state composition, the accumulated solutes prevent solute redistribution and the solute concentration in the entire casting should be equal to the initial value and remain constant during OCC process because solute diffusion is a very slow process.

Thus the solute diffusion coefficient, D_i , of the macroscopic solute transport in Eq(11) is almost zero, and although the solute will be microscopically be rejected at the S/L interface, there is no mechanism to transport the solute. This same behavior was also shown by Diao and Tsai⁽¹⁵⁾ during directional solidification of an Al-4.1wtCu alloy.

The critical stirring intensity required to produce ingots of highest purity during OCC process was obtained from rigorous trial and error using different stirring rates. Figures 9 and 10 shows the solute distribution in ingot and its corresponding axial distribution in presence of optimum stirring intensity (Figure 11) for casting of 2 m ingot. Stirring significantly increased the ingot purity level from 99.77% to above 99.925%Al at the center of the ingot where stirring is effective. The sides of the ingots are a bit less pure due to inefficiency of the stirrer design used. Since the fresh melt will be continuously moving into the heated mold during OCC process, it will dilute the bulk melt and maintains it at a low solute composition for a long time. When the solute level of the ingots becomes higher than the initial alloy being used, then the process should be stopped and the melt discarded for other uses.

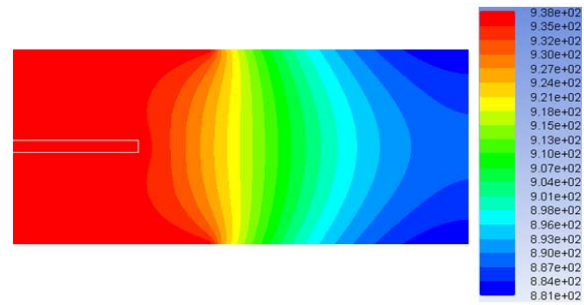


Figure 6. Temperature distribution profile.

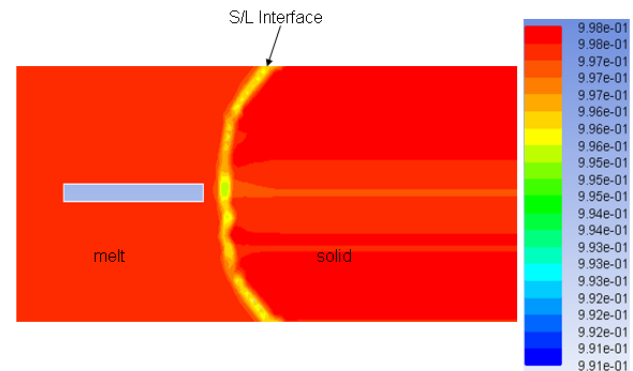


Figure 7. Aluminum redistribution at steady state in absence of melt stirring.

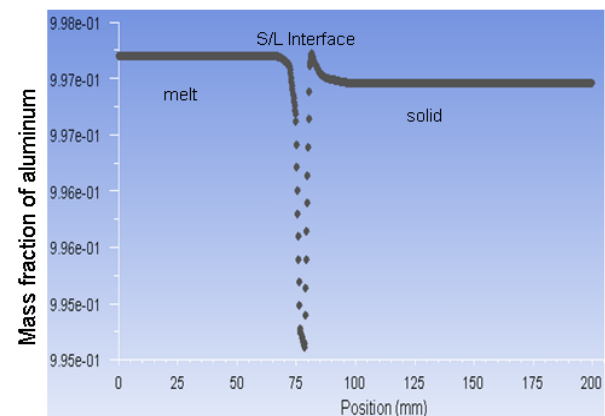


Figure 8. Axial distribution of aluminum in absence of melt stirring.

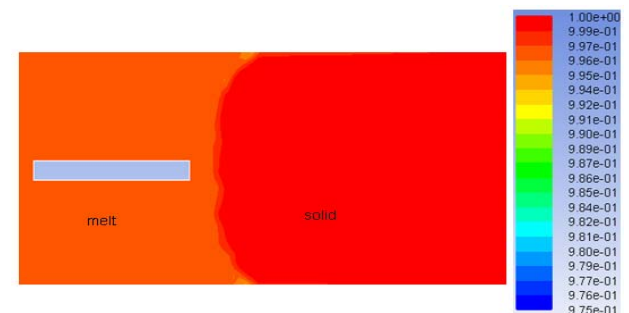


Figure 9. Aluminum redistribution in presence of optimum melt stirring of 10rpm, after casting 2m ingot.

*Purification of an Industrial Aluminum Alloy by Melt Stirring During
Ohno Continuous Casting Process*

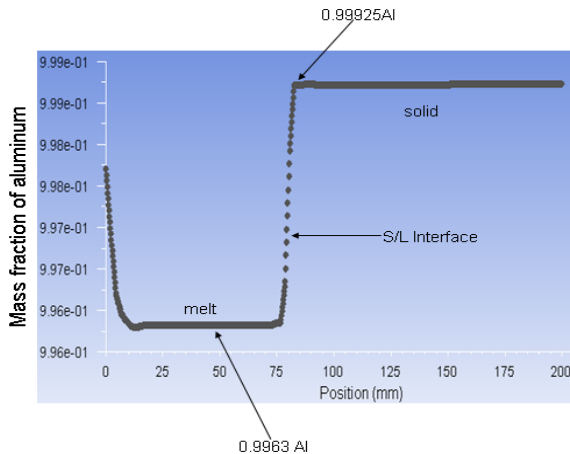


Figure 10. Axial aluminum redistribution at in presence of optimum melt stirring of 10rpm, after casting 2m ingot.

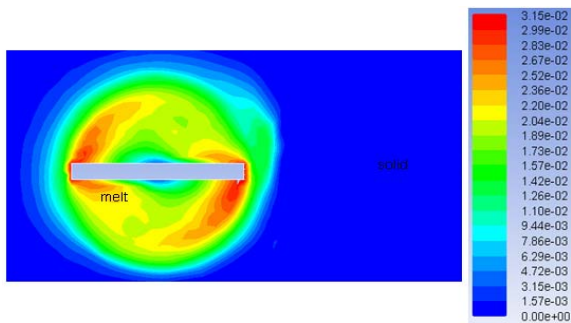


Figure 11. Velocity profile in m/s for optimum mechanical melt stirring of 10rpm.

Conclusions

The critical stirring intensity required under a suitable casting speed to produce aluminum rods of high purity during OCC were determined by numerical simulation. This was done through external stirring of the melt achieved by inserting and rotating a stirrer near the solid-liquid interface to produce a special axial rotating melt flow field of adequate magnitude and direction. The industrial aluminum alloy is very dilute such that very long pure ingots are produced before the purity level falls to below the initial alloy composition. Thus, with optimization of casting speed and stirring intensity, high purity ingots at high production rates are possible to achieve during OCC process. This, of course should be accomplished with a good stirrer design effective in mechanically stirring near the whole interface region.

Acknowledgements

Thanks to Professor Lu. Hao for helpful discussions and provision of CFD Fluent 6.3.26 software.

References

1. Hashimoto, E., Ueda, Y. & Kino, T. (1995). Purification of ultra-high purity aluminum. *J. Phys. IV France* **5(C7)**: 153-157.
2. Jie, W. (2001). Solute redistribution and segregation in solidification processes. *Sci. Technol. Adv. Mat.* **2(1)**: 29-35.
3. Tiller, W.A., Jackson, K.A., Rutter, J.W. & Chalmers, B. (1953). The redistribution of solute atoms during the solidification of metals. *Acta Metall.* **1(4)**: 428-437.
4. Willers, B., Eckert, S., Nikrityuk, P.A., Rübiger, D., Dong, J. Eckert, K. & Gerberth, G. (2008). Efficient melt stirring using pulse sequences of a rotating magnetic field: Part II. application to solidification of Al-Si alloys. *Metall. Mater. Trans. B* **39(2)**: 304-316.
5. Mullin, J.B. & Hulme, K.F. (1958). The use of electromagnetic stirring in zone refining. *Int. J. Electron.* **4(2)**: 170-174.
6. Soda, H., McLean, A., Wang, Z. and Motoyasu, G. (1995). Pilot-scale casting of single-crystal copper wires by the Ohno continuous casting process. *J. Mater. Sci.* **30(21)**: 5438-5448.
7. Ohno, A. (1986). Continuous casting of single crystal ingots by the OCC process. *Journal of Metals* **38(1)**: 14-16.
8. Soda, H., McLean, A., Motoyasu, G. & Ohno, A. (1995). Ohno continuous casting. *Adv. Mater. Process.* **147(4)**: 43-45.
9. Bennon, W.D. & Incropera, F.P. (1987). A continuum model for momentum, heat and species transport in binary solid-liquid phase change systems—I. Model formulation. *Int. J. Heat Mass Tran.* **30(10)**: 2161-2170.

10. Prescott, P.J., Incropera, F.P. & Bennon. W.D. (1991). Modeling of dendritic solidification systems: reassessment of the continuum momentum equation. *Int. J. Heat Mass Tran.* **34(9)**: 2351–2359.
11. Voller, V. R. & Swaminathan, C. R. (1991). ERAL Source-based method for solidification phase change. *Numer. Heat Tr. B-Fund.* **19(2)**: 175-189.
12. Patankar, S.V. (1980). *Numerical heat transfer fluid flow*. NewYork, NY: Hemisphere: 96-102.
13. J.D.Verhoeven, *Trans.AIME.* 242 (1968) 1937-1942.
14. Lee, J.H., Liu, S., Miyahara, H. & Trivedi, R. (2004). Diffusion-coefficient measurements in liquid metallic alloys. *Metall. Mater. Trans. B* **35(5)**: 909-917.
15. Diao, Q.Z. & Tsai, H.L. (1993). Modeling of solute redistribution in the mushy zone during solidification of aluminum-copper alloys. *Metall. Mater. Trans. A* **24(4)**: 963.